

Scale Radii and Aggregation Histories of Dark Haloes

Eduard Salvador-Solé^{*}, Alberto Manrique and José María Solanes

*Departament d’Astronomia i Meteorologia and Centre Especial de Recerca en Astrofísica, Física de Partícules i Cosmologia †
Universitat de Barcelona, Martí i Franquès 1, E-08028 Barcelona, Spain*

8 November 2018

ABSTRACT

Relaxed dark-matter haloes are found to exhibit the same universal density profiles regardless of whether they form in hierarchical cosmologies or via spherical collapse. Likewise, the shape parameters of haloes formed hierarchically do not seem to depend on the epoch in which the last major merger took place. Both findings suggest that the density profile of haloes does not depend on their aggregation history. Yet, this possibility is apparently at odds with some correlations involving the scale radius r_s found in numerical simulations. Here we prove that the scale radius of relaxed, non-rotating, spherically symmetric haloes endowed with the universal density profile is determined *exclusively* by the current values of four independent, though correlated, quantities: mass, energy and their respective instantaneous accretion rates. Under this premise and taking into account the inside-out growth of haloes during the accretion phase between major mergers, we build a simple physical model for the evolution of r_s along the main branch of halo merger trees that reproduces all the empirical trends shown by this parameter in N -body simulations. This confirms the conclusion that the empirical correlations involving r_s do not actually imply the dependence of this parameter on the halo aggregation history. The present results give strong support to the explanation put forward in a recent paper by Manrique et al. (2003) for the origin of the halo universal density profile.

Key words: cosmology: theory – dark matter – galaxies: haloes

1 INTRODUCTION

High-resolution N -body simulations of hierarchical cosmologies with standard cold-dark-matter show that the spherically averaged density profile of relaxed dark haloes in the present epoch is universal. It is always well fitted by the analytical function

$$\rho(r) = \frac{\rho_c r_s^3}{r^\beta (r_s + r)^{3-\beta}} \quad (1)$$

where r is the radius, β the central asymptotic logarithmic slope, with fixed value equal to 1 according to NFW (see also, e.g., Huss, Jain & Steinmetz 1999; Jing 2000; Bullock et al. 2001; Power et al. 2003) or closer to 1.5 according to other authors (e.g., Moore et al. 1998; Ghigna et al. 2000; Fukushige & Makino 2001; Klypin et al. 2001), and ρ_c and r_s the scaling density and radius. Thus, halos with a given mass have density profiles characterised by one single parameter. In fact, the scale radius r_s or the concentration c , defined as R/r_s in terms of the virial ra-

dius R , are found to tightly correlate with halo mass in all the cosmologies studied by NFW, a relationship that is believed to reflect the fact that less massive haloes typically form earlier, when the mean cosmic density is higher (NFW; Salvador-Solé, Solanes & Manrique 1998). Bullock et al. (2001), Wechsler et al. (2002, hereafter WBPkd), and Zhao et al. (2003a, hereafter ZMJB) have both extended these results to other redshifts in the flat Λ CDM cosmology (see also Eke, Navarro & Steinmetz 2001; Zhao et al. 2003b; Tasitsiomi et al. 2004) and provided toy-models for the evolution of r_s .

Within the hierarchical paradigm of structure formation, mergers appear to contribute decisively to the evolution of haloes. For this reason, it seems natural to try to explain the origin of the universal halo density profile focusing on the role of mergers (e.g., Salvador-Solé et al. 1998; Syer & White 1998; Raig, González-Casado & Salvador-Solé 1998; Subramanian, Cen & Ostriker 2000; Dekel, Devor & Hetzroni 2003). While a number of investigations (Avila-Reese, Firmani & Hernández 1998; Nusser & Sheth 1999; Del Popolo et al. 2000; Kull 2000; Williams, Babul & Dalcanton 2004) have demonstrated that NFW-like density profiles can be obtained by simple spherical collapse, it is not clear why this functionality

^{*} E-mail: e.salvador@ub.edu

[†] Associated with the Instituto de Ciencias del Espacio, Consejo Superior de Investigaciones Científicas

should be preserved after major mergers since these events produce an important loss of memory through the rearrangement and violent relaxation of the system. Yet, as shown by numerical experiments, haloes end up with very similar density profiles regardless of whether or not they have undergone major mergers (Huss, Jain & Steinmetz 1999) and, provided they have, regardless of the epoch when the last of these events took place (Moore et al. 1999; WBPKD). The situation is even more confusing when one takes into account that the above mentioned mass-concentration relation and other correlations involving r_s (or c) recently reported by WBPKD and ZMJB (see § 4) suggest, on the contrary, that the structure of haloes depends on their individual aggregation¹ history.

In a recent paper, Manrique et al. (2003, hereafter MRSSS) have shown that the sole hypothesis that haloes grow inside-out with the typical accretion rate of the cosmology under consideration automatically leads to a density profile of the NFW-like form as well as to the mass-concentration relation found at $z = 0$ by NFW in numerical simulations of that cosmology. Moreover, the mass-concentration relation predicted for the Λ CDM universe at different redshifts is also in good agreement with the empirical correlations obtained by Bullock et al. (2001) (MRSSS; Hiotelis 2003). MRSSS argued that the only reasonable explanation for the good predictions of this pure inside-out accretion scheme is that the typical density profile of relaxed haloes is essentially determined by their current mass and the boundary conditions set by the matter that is currently being accreted. In this manner, *relaxed haloes emerging from major mergers would have radial profiles indistinguishable from those of haloes with identical global properties and boundary conditions but having endured a more gentle growth*. This would also explain the fact pointed out by Gao et al. (2004) that some aspects of massive elliptical galaxies imply that haloes evolve by preserving their inner structure as in the pure inside-out accretion scheme (Loeb & Peebles 2003) while they actually experience important rearrangements in major mergers. However, this possibility is apparently in contradiction with the correlations involving r_s (or c) found in numerical simulations.

In the present paper we examine this issue in detail. In § 2, we show that, under some common approximations, r_s depends exclusively on the current values of the halo total mass, energy and the respective instantaneous accretion rates, so there is no room for a dependence on the halo aggregation history. From this result, we develop, in § 3, a simple physical model for the evolution of the scale radius along the main branch of halo merger trees that allows us to show, in § 4, that there is actually no contradiction between the independence of r_s from the halo aggregation history and the correlations found in numerical simulations suggesting the opposite conclusion. Our results are summarised and discussed in § 5. Unless otherwise stated, the cosmology used throughout this paper is the same as in WBPKD and ZMJB studies, that is, a Λ CDM model with $(\Omega_m, \Omega_\Lambda, h, \sigma_8) = (0.3, 0.7, 0.7, 1)$.

2 GENERAL DEPENDENCE OF THE SCALE RADIUS

We will assume hereafter that relaxed haloes are non-rotating and spherically symmetric (see § 5 for a discussion on the implications of these first-order approximations). Taking the potential origin such that $\Phi(R) = -GM/R$, the virial relation adopts the simple scalar form

$$\int_0^R dM(r) \frac{M(r)}{r} = \frac{-2E + 4\pi R^3 P}{G}, \quad (2)$$

where G is the gravitational constant, E the total energy of the halo, P the pressure at the virial radius R and $M(r)$ the mass within r ,

$$M(r) = \int_0^r d\tilde{r} 4\pi \tilde{r}^2 \rho(\tilde{r}). \quad (3)$$

Since the virial radius of a halo at a given cosmic time t is a function of its total mass through the relation

$$R = \left[\frac{3M}{4\pi \Delta_v(t) \bar{\rho}(t)} \right]^{1/3} \quad (4)$$

resulting from the identification of haloes as connected regions with overdensity $\Delta_v(t)$ relative to the mean cosmic density $\bar{\rho}(t)$, it is clear from equation (2) that $\rho(r)$ depends on the three independent quantities M , E and P .

Moreover, as we will see in § 3, relaxed haloes grow inside-out between major mergers, which allows one to express P in terms of the instantaneous mass and energy accretion rates. Indeed, under these circumstances their structure within the instantaneous virial radius at any time t during smooth accretion remains frozen. Then the definition of the total mass (eq. [3] with r equal to R) and the virial relation (eq. [2]) lead to

$$M(t) - M_0 = \int_{R_0}^{R(t)} dr 4\pi r^2 \rho(r) \quad (5)$$

$$2E(t) - 2E_0 = - \int_{R_0}^{R(t)} 4\pi r^2 \rho(r) \frac{GM(r)}{r} dr + 4\pi [R^3(t)P(t) - R_0^3 P_0], \quad (6)$$

where $R(t)$, $M(t)$, $E(t)$ and $P(t)$ are the virial radius, mass, energy and confining pressure of the evolving halo at t and R_0 , M_0 , E_0 and P_0 their respective values at an arbitrary initial epoch t_0 after the last major merger. By differentiating these two equations and taking into account the Jeans equation $dP/dr = -GM(r)\rho(r)/r^2$, we obtain the relations

$$\dot{M} = 4\pi R^2(t) \rho[R(t)] \dot{R} \quad (7)$$

$$\dot{E} = \dot{M} \left\{ -\frac{GM(t)}{R(t)} + \frac{3P(t)}{2\rho[R(t)]} \right\}, \quad (8)$$

from which one can infer, aside from the inside-out evolving density profile (see MRSSS and Hiotelis 2003), the pressure at the instantaneous virial radius

$$P(t) = \frac{\dot{M}}{6\pi R^2(t) \dot{R}} \left[\frac{\dot{E}}{\dot{M}} + \frac{GM(t)}{R(t)} \right], \quad (9)$$

where \dot{R} is a known function of M , \dot{M} and t following from the differentiation of equation (4) with R and M some functions of t .

¹ Throughout the present paper, we use the word ‘‘aggregation’’ to refer to halo growth through mergers of any strength and reserve the word ‘‘accretion’’ for growth due to minor mergers only.

Thus, the density profile $\rho(r)$ of relaxed haloes at t depends on the four independent quantities: M , E , \dot{M} and \dot{E} , fixing the right hand-side member of equation (2). Of course, these are not the only variables on which $\rho(r)$ may depend since the uniqueness of the solution of equation (2), regarded as an integral equation for $\rho(r)$, is not warranted in general (not even in the case that $\rho(r)$ can be restricted, once M is fixed, to a one-parameter function). Therefore, $\rho(r)$ may in principle depend on other quantities, perhaps related to some aspects of the aggregation history of the halo as the correlations mentioned in § 1 suggest. In Appendix A, we show however that for density profiles of the NFW-like universal form the solution of equation (2) is unique. Consequently, the only parameter required to fix the density profile in this case, r_s , must depend exclusively on M , E , \dot{M} and \dot{E} . In other words, *all relaxed (spherical, non-rotating) haloes with identical current values for these four independent quantities necessarily have the same value of r_s regardless of their individual aggregation history.*

A first implication of this result is that it allows one to understand the origin of the mass-concentration relationship shown by haloes at any given epoch without the need to presume any dependence of r_s on the time of their formation. As we have just shown, r_s (or c) depends, at a given t , on M , E , \dot{M} and \dot{E} , while the latter three quantities are expected to correlate, in any given cosmology, with M . To see this latter point we must take into account that the kinetic energy of protohaloes at some early enough, otherwise arbitrary, time t_i arises essentially from the Hubble flow at that epoch, whereas their potential energy should not be far from that of a peak of density contrast

$$\delta_i = \delta_c \frac{D(t_i)}{D(t)} \quad (10)$$

on the scale

$$R_i = \left[\frac{3M}{4\pi \bar{\rho}(t_i)} \right]^{1/3}, \quad (11)$$

with the most probable density profile (Bardeen et al. 1986). In equation (10), δ_c is the linearly extrapolated density contrast for spherical collapse at the present time (equal to 1.69 in an Einstein-de Sitter universe) and $D(t)$ the, also cosmology-dependent, linear growth factor. Thus, once the arbitrary time t_i is fixed, equations (10) and (11) can be used to estimate the (conserved) total energy E of haloes as a function of M and t . On the other hand, the mass accretion rate \dot{M} of haloes at t is well approximated by (Raig, González-Casado, & Salvador-Solé 2001)

$$r_a(M, t) = \int_0^{\Delta_m M} \Delta M r_{\text{PS}}(M, \Delta M, t) d\Delta M, \quad (12)$$

where $r_{\text{PS}}(M, \Delta M, t)$ is the usual Extended Press-Schechter (EPS) merger rate (Lacey & Cole 1993) and Δ_m is the fractional mass increase above which a merger is considered major and, therefore, does not contribute to accretion anymore (Salvador-Solé et al. 1998). Finally, by introducing the former two functions, $E(M, t)$ and $\dot{M}(M, t)$, into the fundamental relationship

$$\dot{E}(M, t) = \frac{\partial E}{\partial M} \dot{M} + \frac{\partial E}{\partial t}, \quad (13)$$

one can also estimate the energy accretion rate \dot{E} in terms of M and t .

We want to stress that this interpretation leads to quantitative predictions of the mass-concentration relation from the EPS theory that are, except for rare very massive haloes, in good agreement with the results of N -body simulations for different cosmologies and redshifts (MRSSS; Hiotelis 2003).

3 A PHYSICAL MODEL FOR THE EVOLUTION OF r_s

We have just seen that the mass-concentration relation can be explained without presuming any dependence of the density profile of haloes on their mass aggregation history. In § 4, it will be shown that the same is true with regards the correlations reported by WBPkd and ZMJB. But to do this we need first to determine how r_s evolves along the main branch of halo merger trees.

In § 2 it was assumed that, during the gentle accretion phase between major mergers, relaxed haloes grow inside-out, i.e., their inner structure remains frozen. This implies that haloes evolving along typical accretion tracks, represented by the solution of the differential equation (Raig et al. 2001)

$$\frac{dM}{dt} = r_a[M(t), t], \quad (14)$$

where $r_a(M, t)$ is the mass accretion rate given by equation (12), maintain an unaltered value of r_s or, equivalently, that such typical mass accretion tracks coincide with typical r_s -isopleths. Moreover, according to the result of § 2, these r_s -isopleths do not depend on the past evolution of haloes but just on their current mass. Thus, haloes undergoing a major merger will jump from the r_s -isopleth they were initially following to a new r_s -isopleth according only to their change in mass, with the constant value of r_s associated with each accretion track given by the mass-concentration relation at any arbitrary redshift. Therefore, the typical value of r_s for a halo evolving along the main branch of a merger tree is simply that corresponding to the typical r_s -isopleth (or mass accretion track) that is intersected, at each moment, by the Mass Aggregation Track (MAT) followed by the halo.

At this stage, it is important to remark that the key assumption in this scheme, namely that haloes grow inside-out between major mergers, is fully supported by the results of numerical simulations. When a halo evolves through accretion and major mergers, M necessarily increases but r_s may not do so; in periods of inside-out growth, r_s will be kept unaltered. The opposite is not true, of course: the invariance of r_s does not guarantee that the inner structure of the halo remains frozen as the characteristic density ρ_c may vary. What should certainly be a secure signature for the inside-out growth of haloes along the main branch of merger trees is the simultaneous constancy of both the scale radius r_s and the mass M_s interior to it, as these two quantities fix the two degrees of freedom of the NFW-like density profile. In this case, the inner structure remains necessarily frozen and the mass M grows just because R does. Therefore, the inside-out growth of haloes between major mergers must lead to values of r_s and M_s that are kept simultaneously constant

along the main branch of halo merger trees between any two sudden increases of M marking major mergers. As Figures 2 and 3 of ZMJB illustrate, this schematic behaviour is indeed found in numerical simulations (see also our Figs. 5 and 6 below where we depict the results of Monte Carlo simulations built under the assumption of halo inside-out growth during the accretion phases). It is not inconsistent either with the results obtained by Gao et al. (2004) from numerical simulations of cluster-sized haloes showing that most of the matter that ends up, at $z = 0$, near the centre is not at the centre of their main progenitor at $z = 4$. The reason is that the inside-out growth only holds between major mergers, while the last major merger where current cluster-sized haloes were rearranged took place at a redshift much smaller than 4 (typically at $z \approx 1$).

From Figures 2 and 3 of ZMJB (and Figs. 5 and 6 below) it is also apparent that the phases of inside-out growth are only found at relatively low redshifts. There is nothing strange in this behaviour. The inside-out growth of a halo during spherical infall is strictly warranted provided only that the orbital period of particles in any given shell is much smaller than the characteristic time of mass infall (see MRSSS and references therein) or, equivalently, that accretion is slow enough. In periods of fast accretion, shell-crossing is expected rather to induce the violent relaxation of the halo just as major mergers do. As one goes back in time, the orbital period of particles in the outermost shell becomes of the order of, and even larger than the typical infall time of accreted matter in the cosmology considered, so the conditions for inside-out growth no longer hold. The redshift z_a at which the transition between fast and slow accretion regimes typically occurs can thus be estimated by comparing the orbital period of particles at the virial radius of the relaxed halo,

$$\tau = \left[\frac{4}{3} \pi G \Delta_v(t) \bar{\rho}(t) \right]^{-1/2}, \quad (15)$$

with the characteristic time of mass infall during accretion, equal to $M/r_a(M, t)$. Thus, given the equality $\bar{\rho}(t) = 3H^2(t)\Omega_m(t)/(8\pi G)$, where $H(t)$ and $\Omega_m(t)$ are respectively the Hubble and density parameters at t , and that, in the relevant range of cosmic times, $\Omega_m(t)$ and $\Delta_v(t)$ can be respectively approximated by 1 and 200 (for $\Delta_v(t)$ according to Bryan & Norman 1998, for which $\Delta_m \sim 0.21$; Hiotelis 2003), the condition for slow accretion adopts the form

$$r_a[M(t), t] \ll 10 H(t) M(t). \quad (16)$$

In Figure 1, we show the redshifts z_a at which the typical mass accretion rates encountered along MATs corresponding to different halo masses satisfy the equality $r_a[M(t), t] = 1.2H(t)M(t)$, where the factor 1.2 has been chosen to give the best agreement with the results of ZMJB (see § 4.2).

According to the previous discussion, the typical r_s -isopleths strictly correspond to the typical evolutionary tracks followed by haloes during *slow* accretion. That is, to infer them we must solve equation (14) taking into account only the slow contribution to the accretion rate. Therefore, for $z \leq z_a$ where accretion is typically slow, the typical r_s -isopleths will coincide with the solutions of equation (14) based on equation (12), while, for $z > z_a$ where accretion is typically fast and the contribution of slow accretion to the right hand-side member of equation (14) is null, they will

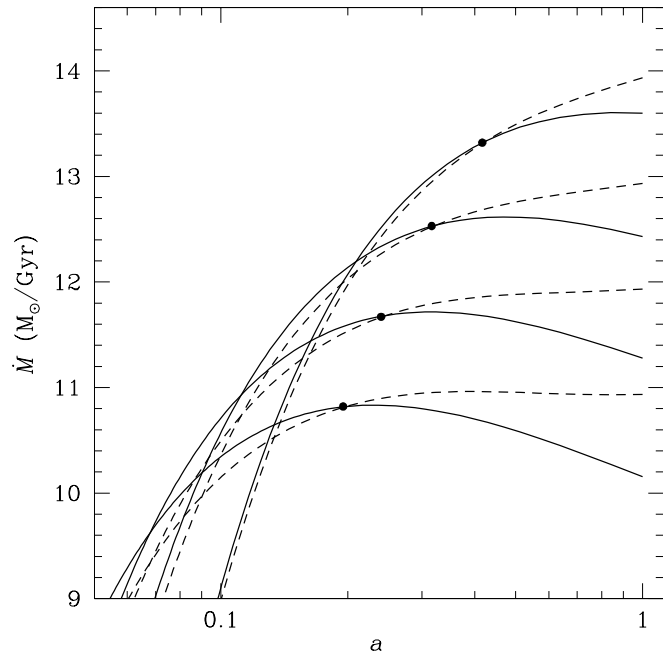


Figure 1. Typical mass accretion rates (solid lines) compared with the quantity $1.2 H(t) M(t)$ (dashed lines) found along the typical main branch of halo merger trees, here referred to as MATs, leading at $z = 0$ to halo masses equal to 10^{12} , 10^{13} , 10^{14} , and $10^{15} M_\odot$ (from bottom to top) for the same cosmology used by ZMJB and WBPkd. The typical MAT corresponding to each halo mass is drawn from equation (18) for the appropriate value of α according to WBPkd. The epoch during which each pair of curves intersects (big dots) gives the characteristic redshift z_a separating the fast and slow accretion regimes in the corresponding MATs.

be kept frozen to the values reached at z_a (see Fig. 2). In this manner, our model for the typical evolution of r_s along MATs becomes valid *at all redshifts*. Note that, compared to other prescriptions for the evolution of r_s available in the literature, our model stands out for being physically motivated and for eliminating the requirement of knowing (and, hence, of storing) the individual aggregation histories of haloes in order to infer the typical value of their r_s at any moment since this is estimated from their current mass only².

Given that the inner structure of haloes, determined by the values of r_s and M_s , is kept unaltered along slow mass accretion tracks, the typical r_s -isopleths coincide, of course, with the typical M_s -isopleths. The constant value of M_s associated to an r_s -isopleth can be obtained from the constant value of this latter parameter and the mass of the halo at any arbitrary time along that track from the relation

$$M_s = \frac{(\ln 2 - 1/2)M}{\ln[1 + R(M)/r_s] - [R(M)/r_s]/[1 + R(M)/r_s]}, \quad (17)$$

arising from the NFW universal density profile, with $R(M)$

² A FORTRAN programme that computes the typical r_s value for relaxed haloes in CDM cosmologies according to our prescription can be downloaded from <http://www.am.ub.es/cosmo/gravitation.htm>

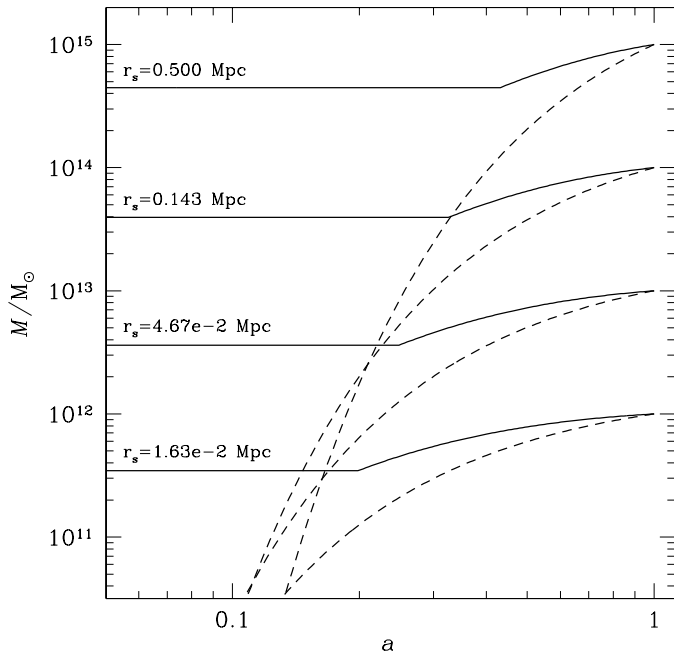


Figure 2. Typical r_s (and M_s) isopleths (solid lines) for haloes with the same final masses (from bottom to top) as in Figure 1. The r_s values associated with the different curves have been calculated from the mass-concentration relation at $z = 0$ given by Bullock et al. (2001). (The corresponding M_s values are given by eq. [17].) The curved part of each isopleth corresponds to the slow accretion regime, while the horizontal part corresponds to fast accretion. Dashed curves show the typical MATs of haloes for the same final masses.

given by equation (4). (Hereafter we assume eq. [1] with $\beta = 1$; were β different from unity, eq. [17] should be replaced by the corresponding expression.) This coincidence between the r_s - and M_s -isopleths implied by our model leads to an interesting prediction that can be easily checked. The relation between r_s and M_s along the different isopleths defines an $r_s - M_s$ relationship that should be typically satisfied by haloes regardless of their mass and redshift. Such a relationship can be obtained from equation (17) and the mass-concentration relation *at any arbitrary redshift*. Therefore, we are led to the conclusion that the $r_s - M_s$ relations inferred from the mass-concentration relations at different redshifts must overlap. (Note that this conclusion is independent of the form of the r_s - or M_s -isopleths and the exact value of β .) In Figure 3, we plot the $r_s - M_s$ relations that result from the empirical mass-concentration relations obtained by Zhao et al. (2003b) at different redshifts, as well as those calculated, for the same redshifts and Λ CDM cosmology, from the toy-models provided by Bullock et al. (2001) and Eke et al. (2001). In the latter two cases, the $r_s - M_s$ relations at different redshifts are all very similar, indeed, confirming our expectations. There is only a slight shift with z which can be attributed to the inherent inaccuracy of the toy-models. However, in the case of Zhao et al., the $r_s - M_s$ relations show a substantial z -dependence. This discrepancy between the behaviours of the $r_s - M_s$ relations derived from the mass-concentration relations provided by

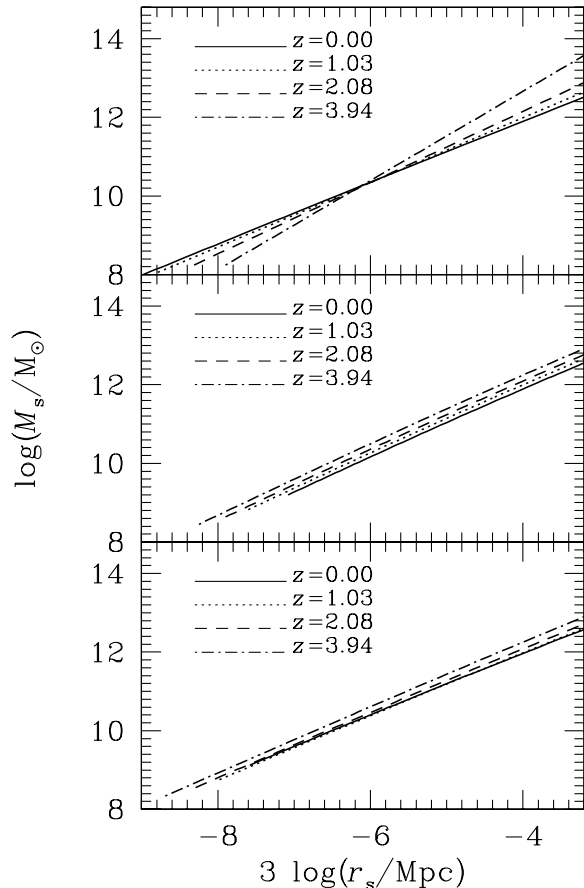


Figure 3. Typical $r_s - M_s$ relations obtained from the mass-concentration relations at different redshifts drawn from Zhao et al. (2003b) data (top) and from the toy models provided by Eke et al. (2001) (center) and Bullock et al. (2001) (bottom) for the same Λ CDM cosmology as in Zhao et al. (2003b), identical to that used throughout the rest of the paper (and in WBKPD and ZMJB studies as well) but for the normalisation constant σ_8 , here equal to 0.9.

different authors is not unexpected given the notable deviation of the mass-concentration relations of Zhao et al. from those of the other two groups at high z (see Fig. 2 of Zhao et al. 2003b). The origin of such a deviation is unclear and deserves further investigation. We note however that the Zhao et al. mass-concentration relations traced by the points drawn from their $25 h^{-1}$ Mpc size box simulation, with softening length equal to $2.5 h^{-1}$ Kpc, closely follow those of the other two groups inferred from simulations with similar softening lengths (equal to 1.8 and $0.4 h^{-1}$ Kpc in Bullock et al. and Eke et al., respectively), while the discrepancy begins to be apparent and becomes definitely marked when the Zhao et al. mass-concentration relations are traced by the points drawn from their 100 and $300 h^{-1}$ Mpc size box simulations, with softening lengths respectively equal to 10 and $30 h^{-1}$ Kpc.

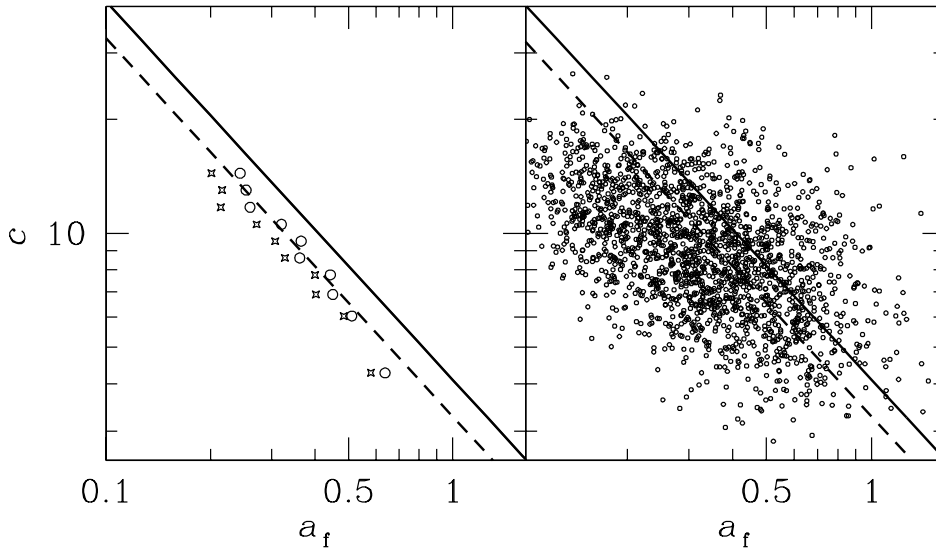


Figure 4. The $c - a(z_f)$ correlation obtained from 2000 Monte Carlo MATs derived in the framework of the EPS formalism using our physical model for the evolution of r_s for haloes with masses (at $z = 0$) larger than $1.43 \times 10^{12} M_\odot$. The quantity a_f plotted in the right panel is the normalized cosmic expansion factor, $a(z_f)/a(0)$, corresponding to the redshift of formation, z_f , of each halo obtained in the way prescribed by WBPKD (see text) from its individual MAT, whereas in the left panel it is the typical value (mean identified by circles and median by crosses) for haloes in final mass bins of 200 objects. The straight lines show the best linear fit to the correlation obtained from N -body simulations by WBPKD (solid line) as well as its shift (dashed line) so to fit the correlation obtained by the same authors from Monte Carlo simulations using their toy-model for r_s that assumes some dependence of this parameter on the individual halo MAT.

4 REINTERPRETING SOME EMPIRICAL CORRELATIONS

4.1 The c vs. α correlation

WBPKD showed that the MAT³ of individual haloes of mass M_0 at a redshift z_0 (as well as the average MAT of haloes with M_0 at z_0) is typically well fitted by the function

$$M(z) = M_0 \exp \left\{ -\alpha \left[\frac{a(z_0)}{a(z)} - 1 \right] \right\}, \quad (18)$$

with $a(z)$ the cosmic scale factor at the redshift z . Thus, by defining the redshift z_f of formation of haloes as the epoch in which the logarithmic slope of their respective MAT takes some fiducial value S (~ 2), the previous result implies the following relation between z_f and α

$$\alpha = \frac{a(z_f)}{a(z_0)} S. \quad (19)$$

In addition, these authors found that the concentration c of haloes at a given redshift correlates with their redshift of formation or, equivalently, with the parameter α associated to their individual MAT. From this result, WBPKD concluded that the density profile of haloes is determined by their aggregation history.

There is a different possibility, however. As shown in § 2, mass and energy conservation, together with the fact that, in any given cosmology, the typical accretion rate of haloes is a function of M and t , allows one to relate the concentration c

of haloes at some given redshift to their mass. This implies, in turn, that c also correlates with any arbitrary function of M , in particular with $\alpha(M)$ giving the typical (mean or median) value of α for haloes of mass M . Since the individual values of α obviously scatter around their typical one, the $c - \alpha(M)$ correlation arising from the mass-concentration relation will induce a secondary correlation between c and the α value corresponding to each MAT or, equivalently, with its associated $a(z_f)$ value. In other words, the $c - a(z_f)$ correlation reported by WBPKD might simply be a consequence of the well-known mass-concentration relation and, just like it, might not imply any dependence of r_s on the aggregation history of haloes.

To check the validity of this alternative explanation we ran 2000 Monte Carlo MATs for present-day haloes with masses according to the Sheth & Tormen (1999) mass function and satisfying the same restriction, $M > 1.43 \times 10^{12} M_\odot$, as in WBPKD and followed, in each, the evolution of r_s predicted by the model developed in § 3 that does not presume any dependence of this parameter on the halo aggregation history. These Monte Carlo MATs were built from the conditional probability that haloes of a given mass at a given epoch arise from smaller objects at earlier epochs given by the EPS theory (Lacey & Cole 1993). The time steps adopted were small enough to ensure the inclusion of only one merger with ΔM above the mass resolution of the simulations according to Lacey & Cole (1993). In this way, to be sure that the inferred MATs really correspond to the main branch of merger trees, we only had to impose that the relative mass increase in any time step was smaller than unity. The values of r_s corresponding to the different isopleths in our physical model for the evolution of this pa-

³ WBPKD did not distinguish between minor and major mergers and used the word accretion for what is here referred to as aggregation.

parameter were drawn from the mass-concentration relation at $z = 0$ of Bullock et al. (2001).

In Figure 4, we show the $c - a(z_t)$ correlation at $z = 0$ obtained from these Monte Carlo simulations. To compensate for the fact that our model for r_s does not include random deviations of E , \dot{M} and \dot{E} from their typical values that depend exclusively on M and t , we have added, according to Jing (2000), Gaussian deviates in $\log(c)$ with a dispersion equal to 0.09. The main trend of this correlation reproduces satisfactorily that found in WBPkd’s N -body simulation (see their Fig. 6). The only small differences concern the slightly larger scatter and the small shift (a little more marked in the medians than in the means) in the Monte Carlo correlation relative to the N -body one. This behaviour is identical to that shown by the correlation obtained by WBPkd in the Monte Carlo simulation they performed, using a slightly different implementation of the EPS theory, to check the validity of their toy-model for r_s that includes an explicit dependence of this parameter on the individual halo MAT. These authors found, indeed, a scatter systematically larger (by 25%) in the Monte Carlo correlation than in the N -body counterpart and the correlation itself shifted exactly by the same amount as found in the present work. As mentioned by these authors, the small deviations of the Monte Carlo predictions with respect to the N -body results are likely caused by the well-known inaccuracies of the EPS formalism (and its practical implementation; see e.g. Somerville & Kolatt 1999 and Raig et al. 2001). In any case, what is important here is that our physical model for r_s is capable of recovering the correlation found by WBPkd at the same level as their toy-model despite the fact that, unlike their model, ours does not presume any dependence of r_s on the halo aggregation history.

4.2 The M_s vs. r_s correlation

ZMJB recently found that haloes show a tight correlation between the r_s and M_s values scaled to those of the main progenitor at a redshift z_{tp} where the MAT shows a characteristic change of slope⁴, which they interpreted as an indication of the passage from fast to slow aggregation regime. Moreover, they showed that the log-log slope of this scaled $r_s - M_s$ correlation changes depending on whether the halo redshift is larger or smaller than the respective z_{tp} value. This finding was interpreted as evidence that the inner structure of haloes depends on their aggregation history. Still, ZMJB did not offer any explanation neither for the origin of this correlation nor for its dependence on the halo redshift relative to z_{tp} .

In fact, the frequency of major mergers cannot be held responsible for the change of slope in the MAT of a halo at z_{tp} because, in the Λ CDM cosmology, major mergers are, for the present-day halo masses considered by ZMJB ($\sim 10^{13} M_\odot$), even more frequent in the slow than in the

fast aggregation regimes defined according to the heuristic redshift z_{tp} . What could explain, instead, the characteristic change of slope in MATs observed at that redshift is the transition from fast to slow *accretion* at z_a mentioned in § 3. Besides, the correlation between r_s and M_s predicted by the model developed in that section is expected to split into two tight correlations similar to those found by ZMJB when the values of the two quantities are scaled to those of the main progenitor at z_a . Note that the $r_s - M_s$ relation shown in Figure 3 is very nearly linear in log-log. Therefore, the fact that major mergers and fast accretion tend to increase with decreasing redshift the values of r_s and M_s as haloes evolve along MATs plus the slight z -dependence of the slope of the log-log $r_s - M_s$ correlation derived from the Zhao et al. (2003b) mass-concentration relations (see Fig. 3) will translate into a small bending (on top of the slight intrinsic one; see Appendix B) of the log-log $r_s - M_s$ correlation shown by haloes along MATs. Consequently, by scaling the values of r_s and M_s to those of the main progenitor at z_{tp} (or z_a) along each individual MAT, such a bent correlation will split into two essentially linear relations on both sides of that redshift, with that corresponding to the fast regime being slightly steeper as found by ZMJB. Note however that, according to our model, since the values of r_s and M_s do not depend on the particular MAT the haloes have followed, the scaled $r_s - M_s$ correlations reported by ZMJB should not rely on their scaling by the specific values of r_s and M_s corresponding to the main progenitor found at z_{tp} (or z_a) along each *particular* MAT. Using as reference the object found at z_{tp} (or z_a) along the *typical* MAT for haloes with the mass of that being studied should yield essentially the same results.

The validity of our interpretation of the ZMJB findings can be checked, like in the case of the WBPkd correlation, by means of Monte Carlo simulations. Unfortunately, this is not so immediate in the present case. As explained in § 3, our model for the evolution of r_s (and M_s) is not fully consistent with the mass-concentration relations found by Zhao et al. at high redshifts. However, we can still check it on the scaled $r_s - M_s$ correlation arising from the mass-concentration relations of Bullock et al. (2001) or Eke et al. (2001) that do not suffer from this problem. As, in the latter case, the general $r_s - M_s$ correlation does not depend on z , we do not expect its z -induced bending along MATs. But, as shown in the Appendix B, this general correlation still has some intrinsic, less marked, convexity, which will also make it split, when properly scaled, into two linear correlations similar to those found by ZMJB, with the reference halo in the individual or typical MATs playing exactly the same role.

With this aim, we performed Monte Carlo MATs as explained in § 4.1 but now following also the evolution of M_s . In Figures 5 and 6 we show a few of these realisations for final halo masses similar to those appearing in Figures 2 and 3 of ZMJB. To better mimic the ZMJB results, the mass increases produced along the MATs were accumulated between each couple of consecutive output times chosen identical to those in the ZMJB N -body simulations. The z_{tp} values, marked on these tracks by arrows, were obtained following the prescription given by ZMJB, whereas the z_a values, marked by big dots, were calculated using the same criterion as in Figure 1. Despite the fact that our r_s and M_s tracks do not include the effects of the random devia-

⁴ The discontinuity in the MAT slope coincides with a maximum or “turning-point” in the function $\log(v_c) + 0.25 \log[H(z)]$, where v_c is the circular velocity of the halo along its MAT, which provides a well-defined practical procedure to determine z_{tp} . Note also that, like WBPkd, ZMJB used the word *accretion* for what is here referred to as *aggregation*.

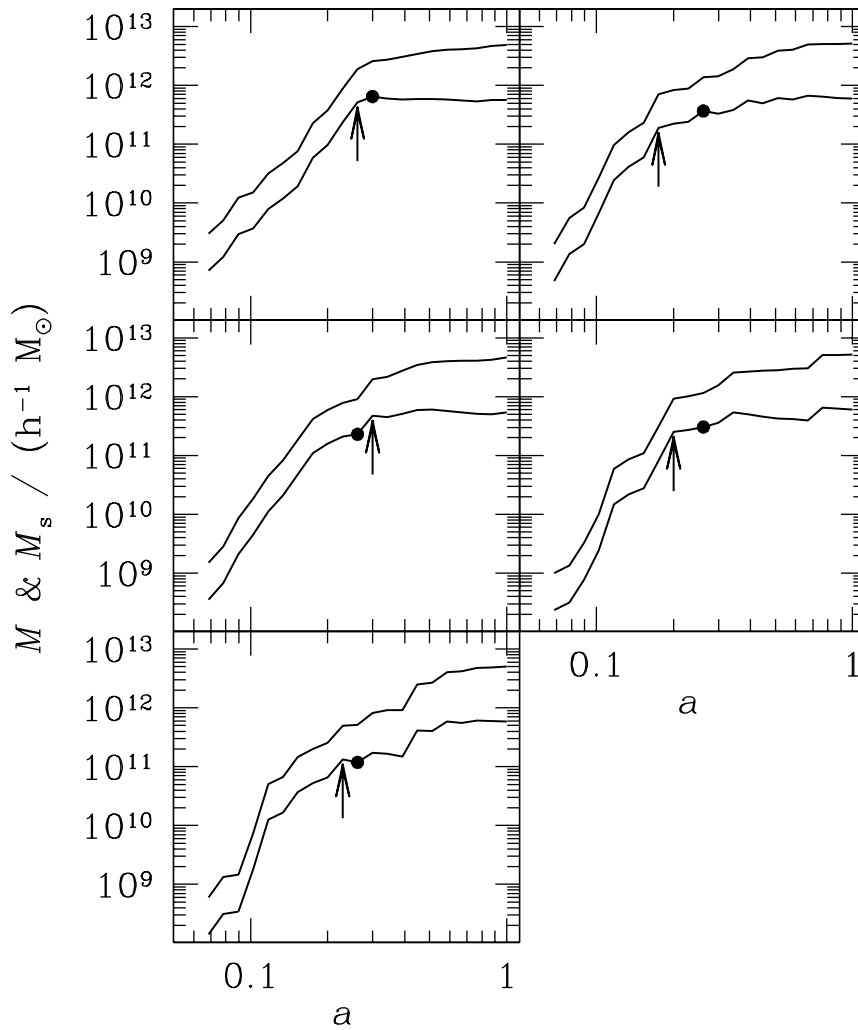


Figure 5. Monte Carlo realisations (upper curves) of MATs and the corresponding M_s tracks (lower curves) derived from the values of r_s plotted in Figure 6 for the same cosmology and similar final halo masses as in ZMJB. The location of the redshift z_a (big dots) marking the typical frontier between fast and slow accretion regimes is compared to the redshift z_{tp} (indicated by arrows) marking the characteristic knee in the mass aggregation tracks indicated by ZMJB. To compare with Figure 2 of ZMJB.

tions of E , \dot{M} and \dot{E} from their respective typical values, they show a remarkable similarity to those depicted in Figures 2 and 3 of ZMJB. There is good agreement not only in the general shape of the MATs and the associated r_s and M_s tracks (see, in particular, the effects of inside-out growth during slow accretion), but also in the typical location of the z_{tp} values. From these figures we can see that every z_{tp} is close to the corresponding z_a marking the change of accretion regime along each MAT, which confirms our guess on the origin of the change in slope of MATs. It is interesting to note that the procedure followed to determine z_{tp} tends to locate this characteristic redshift just after a major merger or an interval of fast accretion. This introduces a systematic discontinuity in the slope of the MATs at that redshift that explains the two-branch analytical fitting formula proposed by Zhao et al. (2003b) for the average MAT of haloes. However, when z_{tp} is not privileged as in WBPkd, the typical MAT of haloes of mass M shows no such discontinuity.

In Figure 7, we plot the scaled $r_s - M_s$ correlations corresponding to the fast and slow accretion regimes, as in Figure 7 of ZMJB, drawn from objects along the Monte Carlo MATs of Figures 5 and 6 at the same redshifts as in the ZMJB figure. To mimic the effects of the random deviations of E , \dot{M} and \dot{E} in N -body haloes, we have added once again Gaussian deviates in $\log(c)$ with a dispersion equal to 0.08 and 0.12 in the slow and fast accretion regimes, respectively. (Unlike WBPkd, who impose no restriction on their halo sample, ZMJB chose relatively isolated final haloes. Hence, the dispersion in c of these haloes is expected to be slightly smaller at $z < z_a$ than in the case of WBPkd. On the contrary, the fact that haloes should be typically less relaxed at $z > z_a$ should cause a higher dispersion in c there.) In the top panels, we show the results obtained when the scaling reference is the halo located at z_a along the *typical* MAT for the mass of each object, while in the bottom panels we show those obtained by using, instead, the halo at z_{tp} along

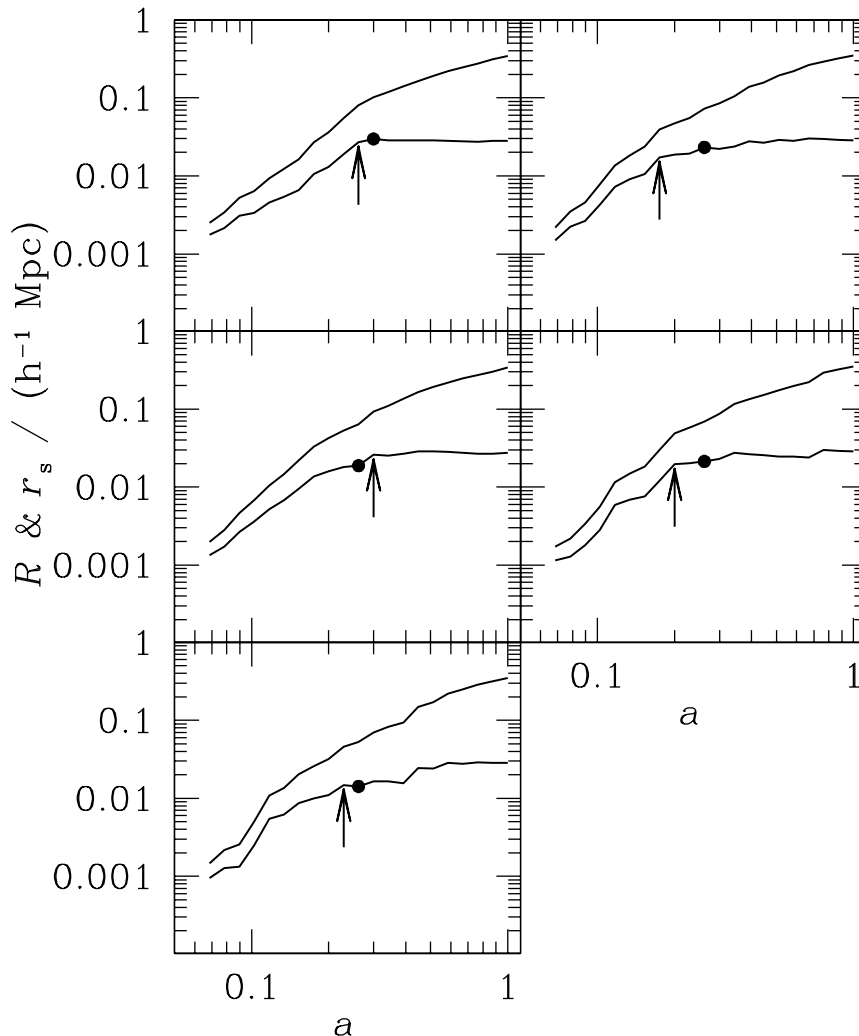


Figure 6. Evolving virial radii R (upper curves) and scale radii r_s (lower curves) predicted by our physical model for the evolution of this parameter corresponding to the Monte Carlo MATs plotted in Figure 5. To compare with Figure 3 of ZMJB.

each *individual* MAT just like in ZMJB. As expected, both variants show identical trends: tight linear correlations in log-log with similar slopes and scatters, strongly resembling those in the original ZMJB scaled correlations. Specifically, the slopes in the fast and slow accretion regimes are 0.76 ± 0.03 and 0.65 ± 0.03 , for the typical-MAT variant, and 0.79 ± 0.02 and 0.64 ± 0.03 , for the particular-MAT one. Since in the former case, the correlations obtained do not involve, by construction, the MAT of individual haloes, we conclude that the change in slope of these scaled correlations at z_{tp} (or z_a) does not imply the dependence of r_s (and M_s) on the individual halo aggregation history. The same conclusion should therefore hold for the correlations obtained by ZMJB (with slopes in the fast and slow regimes respectively equal to 0.64 and 0.48).

5 SUMMARY AND DISCUSSION

In the present paper, we have shown that the scale radius r_s of relaxed, non-rotating, spherically symmetric haloes en-

dowed with the universal density profile à la NFW depends exclusively on the current values of their mass and energy and the instantaneous accretion rates of these two quantities. There is therefore no room for any additional dependence on the particulars of their aggregation histories. Using a simple, physically motivated model for the evolution of r_s along the main branch of halo merger trees, we have demonstrated that our finding that r_s does not depend on the halo past evolution is fully compatible with the well-known mass-concentration relation and the correlations recently reported by WBPKD and ZMJB suggesting the opposite conclusion. We note however that the correlation found by ZMJB has an origin slightly different from that predicted within our scheme since it appears to be related to the particular z -dependence of the mass-concentration relation found by these authors compared to that obtained by other groups. The present results support the explanation recently provided by MRSSS for the origin of the universal halo density profile.

Apart from the correlations here investigated, N -

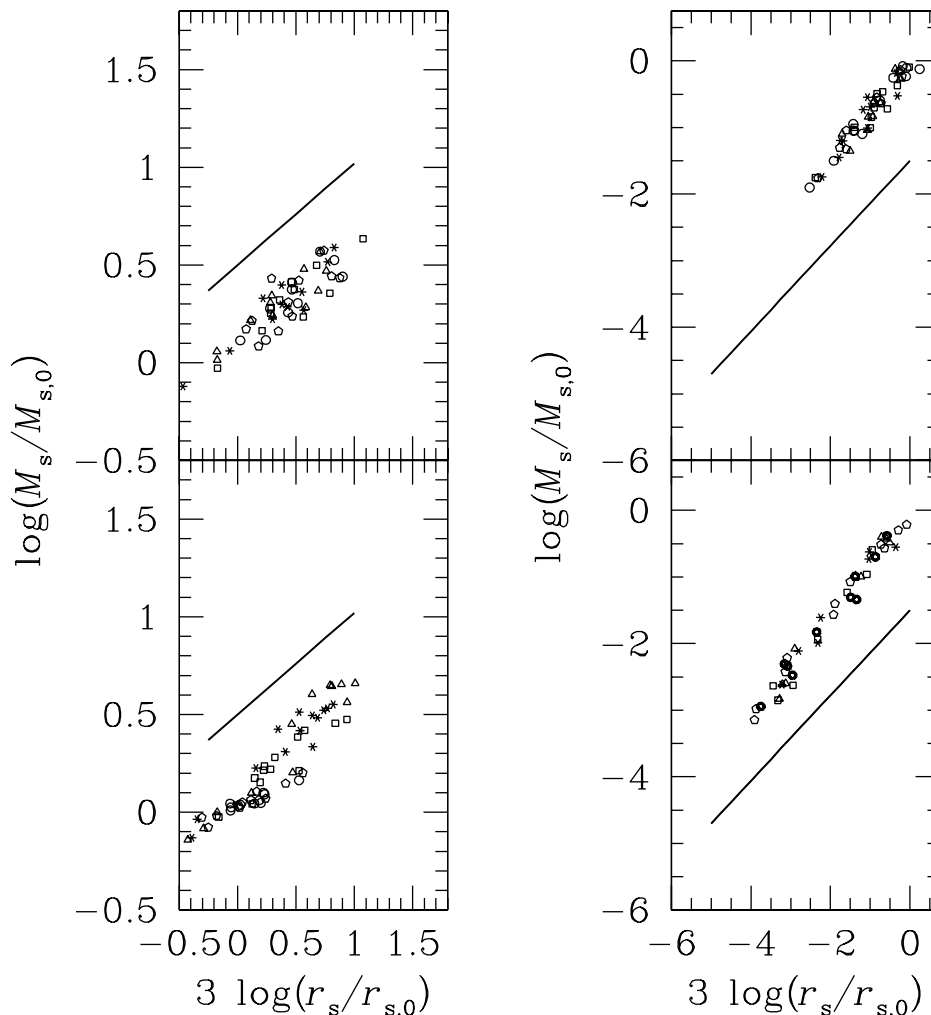


Figure 7. Scaled $r_s - M_s$ correlations drawn from objects along the Monte Carlo MATs shown in Figures 5 and 6 at the same output times of the ZMJB simulations for the slow (left) and fast (right) accretion regimes. The values $r_{s,0}$ and $M_{s,0}$ used to scale the r_s and M_s variables and to separate both aggregation regimes correspond to the halo found at z_a along the typical MAT of each object (top) and to the halo found at z_{tp} along the real individual MAT of each object (bottom). Different symbols are used for objects along different MAT realisations. The straight lines show the slopes of the similar, though with a different origin (see text), empirical correlations found by Zhao et al. (2003b), shifted by the same amount as in their Figure 7.

body simulations show that the density of the local environment also correlates with the frequency of major mergers occurring along the halo aggregation histories (the higher the density, the higher this frequency; Gottlöber, Klypin & Kravtsov 2001) and with the value of r_s (the higher the density, the smaller r_s ; Jing 2000; Bullock et al. 2001). Hence, some correlation may exist between r_s and the frequency of major mergers along the main branch of individual halo merger trees. As is well-known, in its original form the EPS formalism does not contain information on the spatial distribution of haloes, so it is not possible to infer from our model (unless modified along the lines proposed by Mo & White 1996 or Sheth et al. 2001) any correlation between r_s and local density from our model. However, given that the environment of a halo should affect its instantaneous accretion rate (the higher the density,

the larger the typical accretion rate) and that, as we have demonstrated, the value of r_s depends on this latter quantity, a correlation between r_s and local density is also expected to hold within our scheme. For the same reason, the fact that haloes located in high (low) density environments may have had a higher (lower) chance of merging with other haloes along their past history is not inconsistent with the present results either. What these results do not support is the existence of a *direct causal relation* between the frequency of major mergers endured by a halo during its growth and the final value of its scale radius.

The conclusions of the present study rely on some hypotheses that deserve some discussion. The least controversial of these is that of the inside-out growth of haloes between major mergers; as shown in § 3, it is fully supported by the results of numerical simulations. In contrast, the as-

sumption that haloes are spherically symmetric and non-rotating is actually not very realistic. Had we not adopted these simplifying approximations, the angular momentum, the asphericity of the system (via the inertia tensor) and the anisotropy of the local velocity tensor would appear in the full vectorial form of the virial relation, invalidating the proof in Appendix A. We thus cannot discard the possibility that, under more realistic assumptions, the inner structure of haloes can preserve some memory of their aggregation history. We are not concerned here, of course, about the memory embodied in the final value of any extensive property, such as the total mass, energy or angular momentum, that are integrated, and hence fully convolved, over the entire evolutionary history of the system. The kind of memory that is relevant for the present discussion is rather that associated with the possible imprint on the inner structure of haloes of *specific events*, such as the formation of the halo (whatever its definition), the transition from fast to slow aggregation regimes or the frequency of major mergers, having taken place at some point in the past. Certainly, the elongation and the anisotropy of the velocity tensor of haloes indicate that the episodes of violent relaxation do not proceed until completion. But this does not necessarily mean, of course, that the loss of memory produced in those relaxation processes is so small that precise information on those specific events can be recovered from the final properties of the spherically averaged density profile. The results obtained in the present paper rather suggest, along the lines of those drawn from N -body experiments mentioned in § 1 (Huss, Jain & Steinmetz 1999; Moore et al. 1999; WBPkd), that the density profile of haloes is largely insensitive to the details of their aggregation history. In any case, they show that, from the correlations found in numerical simulations, it cannot be concluded that r_s depends on the halo aggregation history since, at least under the assumption of spherical symmetry and null-rotation, they are well explained and quantitatively recovered without presuming such a dependence.

ACKNOWLEDGEMENTS

This work was supported by Spanish DGES grant AYA2003-07468-C03-01. We wish to thank the ZMJB team for kindly providing the data on their mass-concentration relations and James Bullock and Julio Navarro for making publicly available their toy-model codes. We are also grateful to Andrei Doroshkevich and Juan Uson for useful comments.

REFERENCES

- Avila-Reese V., Firmani C., Hernández X., 1998, ApJ, 505, 37
- Bardeen J. M., Bond J. R., Kaiser N., Szalay A.S., 1986, ApJ, 304, 15
- Bryan G. L., Norman M. L., 1998, ApJ, 495, 80
- Bullock J. S., Kolatt T. S., Siyad Y., Somerville R. S., Kravtsov A. V., Klypin A. A., Primack J. R., Dekel A., 2001, MNRAS, 321, 559
- Dekel A., Devor J., & Hetzroni G., 2003, MNRAS, 341, 326
- Del Popolo A., Gambera M., Recami E., Spedicato, E., 2000, A&A, 353, 427
- Eke V.R., Navarro J., Steinmetz M., 2001, ApJ, 554, 114
- Fukushige T., Makino J., 2001, ApJ, 557, 533
- Gao L., Loeb A., Peebles P. J. E., White D. M., 2004, ApJ, 614, 17
- Ghigna, S., Moore, B., Governato, F., Lake, G., Quinn, T., Stadel, J., 2000, ApJ, 544, 616
- Gottlöber S., Klypin A., Kravtsov A. V., 2001, ApJ, 546, 223
- Hiotelis N., 2003, MNRAS, 334, 149
- Huss A., Jain B., Steinmetz M., 1999, ApJ, 517, 64
- Jing Y. P., 2000, ApJ, 535, 30
- Jing Y. P., Suto Y., 2000, ApJ, 529, L69
- Klypin A., Kravtsov A. V., Bullock J. S., Primack J. R., 2001, ApJ, 554, 903
- Kull A., 2000, ApJ, 516, L5
- Lacey C., Cole S., 1993 MNRAS, 262, 627
- Manrique A., Raig A., Salvador-Solé E., Sanchis T., Solanes J.M., 2003, ApJ, 593, 26 (MRSSS)
- Loeb A., Peebles P. J. E., 2003, ApJ, 589, 29
- Mo, H. J., White, S. D. M., 1996, MNRAS, 282, 347
- Moore B., Governato F., Quinn T., Stadel J., Lake G., 1998, ApJ, 490, 493
- Moore B., Quinn T., Governato F., Stadel J., Lake G., 1999, MNRAS, 310, 1147
- Navarro J. F., Frenk C. S., White S. D. M., 1997, ApJ, 490, 493 (NFW)
- Nusser A., Sheth R. K., 1999, MNRAS, 303, 685
- Ostriker J. P., Steinhardt P., 2003, Science, 300, 1909
- Power C., Navarro J. F., Jenkins A., Frenk C. S., White S. D. M., Springel V., Stadel J., Quinn T., 2003, MNRAS, 338, 14
- Press W. H., Schechter P., 1974, ApJ, 187, 425
- Raig A., González-Casado G., Salvador-Solé E., 1998, ApJ, 508, L129
- Raig A., González-Casado G., Salvador-Solé E. 2001, MNRAS, 327, 939
- Salvador-Solé E., Solanes J. M., Manrique A., 1998, ApJ, 499, 542 (SSM)
- Sheth R. K., Tormen G., 1999, MNRAS, 308, 119
- Sheth, R. K., Hui, L., Diaferio, A., Scoccimarro, R., 2001, MNRAS, 325, 1288
- Sommerville R. S., Kolatt T. S., 1999, MNRAS, 305, 1
- Subramanian K, Cen R., Ostriker J. P., 2000, ApJ, 538, 528
- Syer D., White S. D. M., 1998, MNRAS, 293, 337
- Taffoni G., Monaco P., Theuns T., 2003, MNRAS, 333, 623
- Tasitsiomi A., Kravtsov A. V., Gottlöber S., Klypin A., 2004, ApJ, 607, 125
- Wechsler R. H., Bullock J. S., Primack J. R., Kravtsov A. V., Dekel A., 2002, ApJ, 568, 52, (WBPkd)
- Williams L. L. R., Babul A., Dalcanton J. J., 2004, ApJ, 604, 18
- Yoshida N., Springel V., White S. D. M., Tormen G., 2000, ApJ, 544, L87
- Zhao D. H., Mo H. J., Jing Y. P., Börner G., 2003a, MNRAS, 339, 12, (ZMJB)
- Zhao D. H., Jing Y. P., Mo H. J., Börner G., 2003b, ApJ, 597, L9

APPENDIX A: UNIQUENESS OF THE NFW SOLUTION OF THE VIRIAL RELATION

Consider two steady spherically symmetric, non-rotating, self-gravitating systems with identical radius R and total mass M . This obviously warrants that their respective density profiles $\rho(r)$ and $\rho'(r)$ coincide at least at one radius in the open interval $(0, R)$. We next prove that if the two systems also have identical total energy E and are subject to the same external pressure P then the radius at which both profiles coincide cannot be unique.

Suppose that the density profiles $\rho(r)$ and $\rho'(r)$ (assumed with realistic central logarithmic slopes greater than -2 to ensure finite central potentials) do intersect each other at a *single radius* r_e within $(0, R)$. The scalar virial relation (2) allows one to write

$$\int_0^R dM(r) \frac{M(r)}{r} = \int_0^R dM'(r) \frac{M'(r)}{r}, \quad (\text{A1})$$

where $M(r)$ and $M'(r)$ are the mass profiles associated with $\rho(r)$ and $\rho'(r)$, respectively. By integrating by parts both sides of this equality, we obtain

$$\int_0^R dr \frac{M^2(r)}{r^2} = \int_0^R dr \frac{M'^2(r)}{r^2}. \quad (\text{A2})$$

Rewriting equation (A2) in the form

$$\int_0^R dr \left[\frac{M^2(r)}{r^2} - \frac{M'^2(r)}{r^2} \right] = \int_0^R dr [M(r) - M'(r)] \left[\frac{M(r) + M'(r)}{r^2} \right] = 0 \quad (\text{A3})$$

and integrating by parts the second member leads to

$$\int_0^R dr r^2 [\rho(r) - \rho'(r)] J(r) = 0, \quad (\text{A4})$$

where we have introduced the definition

$$J(r) \equiv \int_0^r d\xi \frac{M(\xi) + M'(\xi)}{\xi^2}. \quad (\text{A5})$$

Equation (A4) can be recast in the form

$$\int_0^{r_e} dr r^2 [\rho(r) - \rho'(r)] J(r) = \int_{r_e}^R dr r^2 [\rho'(r) - \rho(r)] J(r), \quad (\text{A6})$$

with the integrands on both sides of equation (A6) being two strictly positive (or negative) functions in the respective open intervals $(0, r_e)$ and (r_e, R) . Since $J(r)$ is a strictly outwards increasing positive function, $J(r_e)$ is, at the same time, an upper bound for $r \in [0, r_e]$ and a lower bound for $r \in [r_e, R]$. Thus, we have the following inequalities

$$\int_0^{r_e} dr r^2 [\rho(r) - \rho'(r)] J(r) < \int_0^{r_e} dr r^2 [\rho(r) - \rho'(r)] J(r_e) \quad (\text{A7})$$

$$\int_{r_e}^R dr r^2 [\rho'(r) - \rho(r)] J(r) >$$

$$\int_{r_e}^R dr r^2 [\rho'(r) - \rho(r)] J(r_e), \quad (\text{A8})$$

which, given equation (A6), lead to

$$J(r_e) \int_0^{r_e} dr r^2 [\rho(r) - \rho'(r)] > J(r_e) \int_{r_e}^R dr r^2 [\rho'(r) - \rho(r)] \quad (\text{A9})$$

or, equivalently, to

$$\int_0^R dr r^2 \rho(r) > \int_0^R dr r^2 \rho'(r). \quad (\text{A10})$$

As inequality (A10) contradicts the fact that the two density profiles must yield the same total mass M , the initial postulate that they coincide at one single radius r_e can be rejected.

Two profiles of the NFW-like form, equation (1), yielding the same mass M , are either identical or intersect at one single intermediate radius r_e in the interval $(0, R)$. Indeed, if they are not identical, they have different values of r_s and of the characteristic density ρ_c , implying that they have different slopes at all radii. This ensures that the function $\rho(r) - \rho'(r)$ has no extreme in the interval $(0, R)$ and, consequently, that it only vanishes once. Thus, according to the previous proof, we conclude that, if at a given epoch two (spherical, non-rotating) relaxed haloes have identical values of R , M , E and P , their density profiles of the NFW universal form must necessarily coincide, too.

APPENDIX B: THE M_s VS. r_s SCALED CORRELATION

Let us neglect, for simplicity, the deviates of E , \dot{M} , and \dot{E} of individual haloes from their typical values dependent on M and t . As explained in § 3, the $r_s - M_s$ relation can be inferred from the mass-concentration relation at any given redshift and equation (17) arising from the universal density profile of haloes. The mass-concentration relation at $z = 0$ given by Bullock et al. (2001) for the same cosmology as in WBPkd and ZMJB leads to the nearly linear $r_s - M_s$ relation in log-log units shown in Figure B1. Should this relation be strictly linear, the r_s and M_s values of haloes would satisfy the relation

$$\log M_s = \alpha_0 + 3\alpha_1 \log r_s. \quad (\text{B1})$$

Since the values $r_{s,0}$ and $M_{s,0}$ of any *arbitrary* halo eventually used to scale the r_s and M_s values of the different objects would also satisfy the relation (B1), we are led to the fact that haloes also show a perfect linear relation (with no scatter) of the form

$$\log(M_s/M_{s,0}) = 3\alpha_1 \log(r_s/r_{s,0}). \quad (\text{B2})$$

However, the real $r_s - M_s$ relation shown in Figure B1 shows a small bending so that haloes rather satisfy the relation

$$\log M_s = \alpha_0 + 3\alpha_1 \log r_s + 3\alpha_2 (\log r_s)^2, \quad (\text{B3})$$

being $\alpha_1 > 0$, $\alpha_2 < 0$ and $|\alpha_2 \log(r_{s,\max}/r_{s,\min})| \ll \alpha_1$, where $r_{s,\max}$ and $r_{s,\min}$ are the upper and lower bounds of r_s in the sample. Given that the values $r_{s,0}$ and $M_{s,0}$ of

any reference halo used to scale r_s and M_s also satisfy the relation (B3), we are led to the scaled relation

$$\log(M_s/M_{s,0}) = 3\alpha_1 \log(r_s/r_{s,0}) + 3\alpha_2 [(\log r_s)^2 - (\log r_{s,0})^2], \quad (\text{B4})$$

which can be rewritten in the form

$$\log(M_s/M_{s,0}) = 3\alpha_1 \left(1 + 2 \frac{\alpha_2}{\alpha_1} \log r_{s,0}\right) \log(r_s/r_{s,0}) + 3\alpha_2 [\log(r_s/r_{s,0})]^2. \quad (\text{B5})$$

Since $|\alpha_2 \log(r_s/r_{s,0})| \ll \alpha_1$, the relation (B5) is well approximated by the linear relation

$$\log(M_s/M_{s,0}) = 3\alpha_1 \log(r_s/r_{s,0}) \times \left\{1 + \frac{\alpha_2}{\alpha_1} \left[2 \log r_{s,0} + \log\left(\frac{r_{s,m}}{r_{s,0}}\right)\right]\right\}, \quad (\text{B6})$$

where $r_{s,m}$ is some intermediate value between $r_{s,0}$ and $r_{s,\max}$ or $r_{s,\min}$ depending on whether r_s is larger or smaller than $r_{s,0}$, respectively. Thus, the slope depends, in this case, on the specific value of $r_{s,0}$ used to scale r_s . Consequently, by taking $r_{s,0}$ equal to the scale radius of some halo along the typical or individual MAT of each object, the slope will slightly change, yielding some scatter in the scaled relation. Note however that this scatter should be very small as $|\alpha_2 \log(r_{s,m}/r_{s,0})/\alpha_1|$ is always much smaller than unity. On the other hand, since $r_{s,m}/r_{s,0}$ is then respectively either smaller or larger than unity, given the signs of coefficients α_1 and α_2 , the slope of the scaled correlation will be systematically larger, though by a small amount, for $r_s \leq r_{s,0}$ than in the case $r_s > r_{s,0}$.

Finally, we do not expect any noticeable difference between the z_a and z_{tp} variants of the scaled correlations. As mentioned in §4, the values of z_a along individual MATs are of the same order as z_{tp} , so their respective values of $r_{s,0}$ should be similar. Certainly, the redshifts z_a correspond to objects along typical MATs, but individual MATs are not very different from the latter. Thus, both variants of the scaled correlations should show essentially the same slope and scatter.

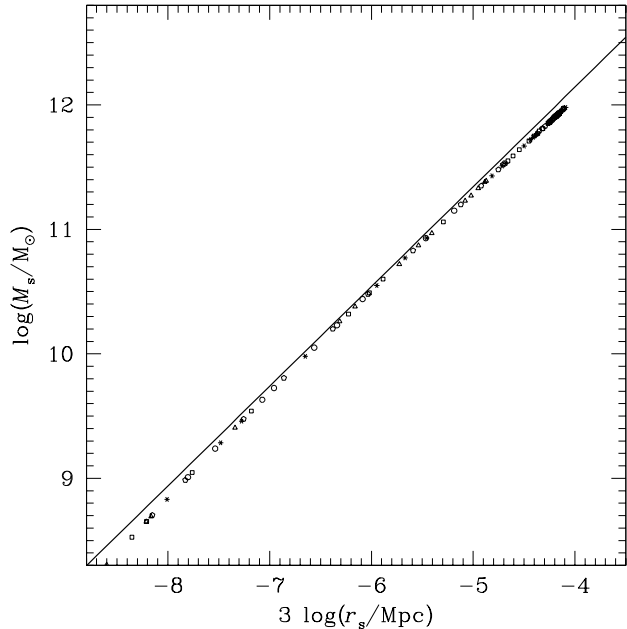


Figure B1. Typical $r_s - M_s$ relation obtained from the same haloes as in Figures 5 and 6 (same symbols as in Figure 7) without adding any scatter in c and prior to the scaling of r_s and M_s and the subsequent splitting in two relations on both sides of the reference halo. To better appreciate the small bending of this relation we show its log-log linear fit (full line) shifted vertically by 0.07.